A Linearly Scaling QM/MM Method to Study Molecular Crystals Using BRABO/CHARMM: Application to 2-(2-Methyl-3-chloroanilino) Nicotinic Acid

Ben Swerts, Joris Van Droogenbroeck, Anik Peeters, and Christian Van Alsenoy*

Structural Chemistry Group, Department of Chemistry, University of Antwerp, Universiteitsplein 1, B-2610 Wilrijk, Belgium

Received: December 13, 2001; In Final Form: February 20, 2002

Molecular crystals have been studied using two new forms of the cluster approach: an extended point charge (PCX) and an extended supermolecule (SMX) model. These models extend, using a hybrid quantum mechanical/molecular mechanical (QM/MM) approach, that part of the molecular environment that was previously described by point charges in, respectively, the point charge (PC) and supermolecule (SM) models. After interfacing the ab initio program BRABO with the molecular mechanics program CHARMM, the PCX and SMX models have been tested on formamide oxime, α-glycine, and the yellow form of dimethyl 3,6-dichloro-2,5-dihydroxyterephthalate. PCX results are in notably better agreement with experimental results than PC results and are shown to be a viable alternative to SM calculations. For α-glycine, the SMX model improves results over the SM model. For dimethyl 3,6-dichloro-2,5-dihydroxyterephthalate, it was shown that the SMX model can give SM-quality results when fewer neighbors are included in the wave function, thereby reducing the computation time significantly. As a second part of this study, the PCX model was applied to the geometry optimization of the four polymorphs of 2-(2-methyl-3-chloroanilino) nicotinic acid. In contrast to a previous study using the PC model, the newly developed PCX model introduced in this study allowed full geometry optimization of all polymorphs.

I. Introduction

Theoretical (ab initio) calculations on crystals can provide valuable information for the experimental determination of crystal structures. The theoretical models introduced in this work are by no means a replacement for these experiments as they start from the experimentally determined space group and lattice parameters. They do, however, provide a faster and easier way to study, for example, hydrogen bonds, mutations of functional groups, or impurities.[1,2] In addition, given a wave function, several properties can easily be calculated.

In the cluster model,[3−6] used for theoretical studies of the solid state, a central molecule is surrounded by identical molecules geometrically arranged in accordance with the applicable space group symmetry. In the past, two forms of this model have been used in studies of the crystal field effects on the geometry of several molecules. In the point charge (PC) model,[7] all surrounding molecules are described by point charges placed on the positions of the atoms. The interaction between the central molecule and its environment is thus treated purely electrostatically. In the computationally more expensive supermolecule (SM) model,[8] the central molecule together with its nearest neighbors are described by a wave function and are surrounded by an outer shell of point charges placed at the more distant atomic positions. This model takes the effect of an overlapping electron cloud between the central molecule and its nearest neighbors into account.

In this study, the PC and SM models are extended to a hybrid quantum mechanical/molecular mechanical[9−11] (QM/MM) description. In these models, designated extended point charge (PCX) and extended supermolecule (SMX) models, respectively, the molecules that were previously described by point charges are now described by a molecular mechanical Hamiltonian. The Hamiltonian for the QM/MM description of a molecular system is

$$H = H_{QM} + H_{MM} + H_{QM/MM}$$

The most commonly used form for the nonbonded QM/MM interaction Hamiltonian consists of an electrostatic and a van der Waals interaction. In cluster calculations, only the central molecule is representative for the molecule in the solid state. For geometry optimizations, the Hamiltonian for the central molecule consequently reduces to

$$H_{central} = H_{QM} + H^{el,stat}{}_{QM/MM} + H^{VdW}{}_{QM/MM}$$

The first two terms describe the PC or SM model. In the new models, the Hamiltonian is extended with a classical van der Waals term. A further difference from the previous approach is the type of charges used. For the PC and SM models, Mulliken[12] or stockholder[13,14] charges were used. In the new models, these are replaced by the standard geometry independent force-field charges. The inclusion of classical van der Waals interactions in a PC model (using ab initio derived charges) is not possible because electrostatic and van der Waals parameters are strongly interdependent. Tests have shown that geometry optimizations using the PC model with force-field charges or using the PCX model with stockholder charges do not lead to satisfactory results.

* To whom correspondence should be addressed. E-mail: alsenoy@uia.ua.ac.be. Fax: +32.3.820.23.10.

10.1021/jp014513j CCC: $22.00
Published on Web 03/26/2002

All models permit the refinement of internal coordinates. The SM and SMX models permit in addition the refinement of external coordinates. Refinement of these coordinates is not possible with the PC model because of a lack of van der Waals repulsion between the central molecule and the point charges. Because of the inclusion of MM-type van der Waals repulsion, the PCX model allows the refinement of these coordinates. Theoretical determination of crystal packing and cell parameters has been studied by several groups[15−17] but will not be pursued in this work.

To obtain a QM/MM code to study molecular crystals using the PCX and SMX models, the ab initio program package BRABO[18] was interfaced with the molecular mechanical package CHARMM.[19] BRABO performs the QM part of the calculation very efficiently, using the linearly scaling MIA method.[18,20] The MM part, which formally scales quadratically,[19] scales linearly if cutoff methods are used for the nonbonded interactions. As such, a linearly scaling QM/MM method is obtained. Moreover, to our knowledge this is the first combination of programs that enables QM/MM type calculations to study molecular crystals.

To assess the performance of the new models, many geometry optimizations have been performed using the PCX and SMX models. In the first part of this study, results for these models have been compared with results obtained using the PC and SM models for three test cases: formamide oxime,[21] α-glycine,[22] and the yellow form of dimethyl 3,6-dichloro-2,5-dihydroxyterephthalate[23] (TERE).

In the second part of this study, the PCX model has been used for the geometry optimization of the four polymorphs of 2-(2-methyl-3-chloroanilino) nicotinic acid[24] (NIC), a molecule which has a medicinal use as an analgesic and antiinflammatory agent. It is an excellent example for the kind of molecules for which the PCX model has been developed; the SM approach is computationally too demanding, whereas the PC model is too simple to describe the interactions of the central molecule with its environment.[25]

II. Computational Details

All structures were optimized using the RHF/MIA method for the central QM molecule or cluster and the CHARMM27 force field for the surrounding MM molecules. Some MM charges were adapted to better reflect the atoms' environments (Tables 18S−21S). In particular for the chlorine atom, which occurs in the molecules TERE and NIC but is not present in the CHARMM27 force field, parameters were based on the values for this atom in the MMFF94[26] force field. Only nonbonded MM parameters were necessary in these applications since the only interactions between the QM and MM regions are nonbonded ones (a complete list of parameters is available as supporting material).

The 6-31G basis set[27] was used for the atoms O, N, C, and H and the 6-6-31G basis set[28] was used for Cl, unless noted otherwise. All surrounding molecules, described by point charges or molecular mechanics, which had at least one atom less than 12 or 20 Å away from the central molecule (the neighbor cutoff), were included in the description of the environment. For formamide oxime and α-glycine, the neighbor cutoff was 12 Å, while for TERE and NIC it was 20 Å. No MM cutoff schemes for nonbonded interactions were used because the structures are small.

Fifteen molecules were included in the wave function in all SM and SMX calculations. For TERE an extra SMX calculation was performed with a supermolecule consisting of 11 molecules.

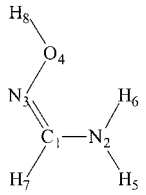

Figure 1. Formamide oxime.

TABLE 1: Standard Deviation of Structural Parameters from Experimental Values for Formamide Oxime Obtained Using the PC, PCX, SM, and SMX Models

parameter	PC	PCX	SM	SMX
bond lengths	0.0166	0.0128	0.0118	0.0117
valence angles	1.55	1.54	1.15	1.15
torsion angles	7.30	3.45	4.32	4.32
out-of-plane angles	10.06	5.39	6.95	6.95

CHARMM acted as the host program calling BRABO at appropriate times. Its CRYSTAL module was used to generate the coordinates of the neighboring molecules according to the space group symmetry at each optimization step. The lattice parameters were constrained to the experimental ones, but the position and orientation of the molecule in the unit cell was refined in the SM, PCX, and SMX models. For NIC−IV, the *z*-coordinate of the center of mass was constrained to the experimental one because that coordinate is undefined in this molecule's space group.

The minimizer program that is part of the BRABO package was added to the list of CHARMM minimizers. This minimizer allows one to perform geometry optimizations in redundant[29,30] as well as nonredundant internal coordinates[31] obtained using a procedure proposed by Pulay. All geometry optimizations for the test cases were performed in nonredundant internal coordinates, while the four polymorphs of NIC were optimized in redundant internal coordinates because of the presence of coupled rings. These procedures strongly reduced the number of optimization steps in comparison with CHARMM's ABNR minimizer as this minimizer performs geometry optimizations in Cartesian coordinates.

All PC and SM results have been obtained using stockholder charges[13] with one exception (see section III.1.c.).

III. Results and Discussion

In the first part of this section, the performance of the PCX and SMX models is evaluated by comparison to the PC[7] and SM[8] models. For the three test cases, only standard deviations from experimental parameters are quoted (Tables 1−3). The space group and lattice parameters for these test cases can be obtained from the experimental studies.

In the second part, the PCX model has been used in a geometry optimization of the four polymorphs of 2-(2-methyl-3-chloroanilino) nicotinic acid (Tables 4−8). Although theoretical (r_e) and experimental (r_α) distances are not strictly comparable, these differences are neglected in this study given the uncertainties of the experimental studies on the title compound.

Cartesian coordinates for all structures are available as supporting material.

III.1. Tests of the PCX and SMX Models. *III.1.a. Formamide oxime.* The results for the geometry optimizations of formamide oxime (Figure 1) are compared to experimental results obtained by neutron diffraction at 15 K[32] in Table 1.

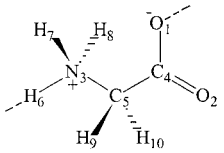

Figure 2. α-Glycine with an indication of its strongest hydrogen-bond interaction in the crystal phase.

TABLE 2: Standard Deviation of Structural Parameters from Experimental Values for α-Glycine Obtained Using the PC, PCX, SM, and SMX Models

Parameter	PC	PCX	SM	SMX
bond lengths	0.0191	0.0083	0.0143	0.0124
valence angles	2.33	0.67	0.83	0.64
torsion angles	23.13	5.95	7.67	4.89
out-of-plane angles	2.92	0.86	1.13	0.75

As can be seen, the PCX model performs significantly better than the PC model. The deviation from experiment for bond lengths and valence angles is intermediate between PC and SM results, but for torsion and out-of-plane angles it is of SM quality. The SMX results show virtually no difference with the SM results. The standard deviations between SM and SMX results for bonds, valence, torsion, and out-of-plane angles are 0.0003 Å, 0.04°, 0.20°, and 0.03°, respectively.

The largest errors for the torsion angles are due to the torsions around the N_2-C_1 bond. This has a direct effect on the corresponding out-of-plane angles.

III.1.b. α-Glycine. The zwitterionic α-glycine molecule proved unoptimizable with the PC model using Mulliken charges as it lead to the transfer of a hydrogen atom resulting in a nonionized molecule[22] (H_6 to O_1 of a neighboring molecule, Figure 2). Using stockholder charges solved this problem, but large discrepancies with experiment[33] remained as can be seen from the first column in Table 2. The standard deviation for torsion angles of 23° could only be reduced to 8° using the SM model. These large errors all arise from the results for torsion angles around the C_5-C_4 bond, which means the COO^- group is rotated with respect to the rest of the molecule, pointing to the fact that the hydrogen-bond interaction (Figure 2) is not adequately described.

Although the deviations for the PCX model are smaller than for the SM model, the large error in the torsion angles is not alleviated. In this case, the SMX model shows a significant improvement. The torsion and out-of-plane angles in particular are in better agreement with experiment.

III.1.c. The Yellow Form of Dimethyl 3,6-Dichloro-2,5-dihydroxyterephthalate. Three polymorphic forms of dimethyl 3,6-dichloro-2,5-dihydroxyterephthalate have been observed,[34,35] with a white, light yellow or yellow color, depending on the molecular conformation and crystal structure. For the yellow form, the ester group is approximately in the plane of the benzene ring. For the white form, it is almost perpendicular to the ring, while the light yellow form shows an intermediate position.

Recently, the yellow form (Figure 3) was studied using the SM model.[23] For a model including 11 molecules in the wave function (SM-11), the ester group rotated 16° out of the plane of the benzene ring. As a result, the closest neighbor to the central molecule was a molecule represented by point charges. When four more neighbors were included in the wave function (SM-15), the molecule remained planar.

For this study, the structure of the molecule has been optimized using the PCX, SMX-11, and SMX-15 models. Because of inclusion of classical van der Waals forces, the molecule remained approximately planar for all models. Previous calculations using the SM model were performed using Mulliken charges. As these results are satisfactory, no recalculation using stockholder charges was performed.

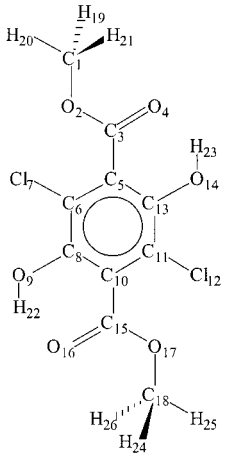

Figure 3. Dimethyl 3,6-dichloro-2,5-dihydroxyterephthalate in its planar yellow form.

TABLE 3: Standard Deviation of Structural Parameters from Experimental Values for the Yellow Form of Dimethyl 3,6-Dichloro-2,5-dihydroxyterephthalate Obtained Using the PCX, SM, and SMX Models

parameter	PCX	PCX**[a]	SM	SMX-15[b]	SMX-11[b]
bond lengths	0.0159	0.0166	0.0203	0.0207	0.0204
valence angles	1.39	0.77	1.30	1.25	1.30
torsion angles	3.63	3.31	0.82	0.80	0.73
out-of-plane angles	1.42	1.02	0.31	0.17	0.16

[a] PCX with the (6-)6-31G** basis set. [b] SMX-A: SMX with A neighbors described by the wave function.

TABLE 4: Experimental Lattice Parameters for the Four Polymorphs of 2-(2-Methyl-3-chloroanilino) Nicotinic Acid

polymorph	space group	NMUC[a]	a	b	c	α	*β*	*γ*
NIC−I	$P2_1/c$	4	7.625	14.201	11.672	90.00	101.65	90.00
NIC−II	$P\bar{1}$	2	13.810	3.858	10.984	94.98	94.42	95.57
NIC−III	$P\bar{1}$	2	7.670	7.254	10.882	100.66	102.02	86.97
NIC−IV	$Pca2_1$	4	23.597	4.042	12.127	90.00	90.00	90.00

[a] The number of molecules in the unit cell.

TABLE 5: Standard Deviation of Structural Parameters from Experimental Values for the Four Polymorphs of 2-(2-Methyl-3-chloroanilino) Nicotinic Acid Obtained Using the PCX Model

parameter	NIC−I	NIC−II	NIC−III	NIC−IV
bond lengths	0.0171	0.0064	0.0096	0.0237
valence angles	0.88	0.89	0.62	1.96
torsion angles	3.67	4.57	1.14	5.28
out-of-plane angles	1.37	1.29	0.80	1.69

The results in Table 3 are obtained from parameters excluding those involving hydrogen atoms, as they cannot be adequately compared to experiment because the experimental values were obtained from an X-ray experiment at room temperature.

The largest error in bond lengths (0.0355 Å) arose from the C−Cl distance, because the 6-6-31G basis set is inadequate to describe the Cl atom. Therefore, a PCX calculation was carried out using the (6-)6-31G** basis set (PCX** in Table 3). Inclusion of polarization functions into the basis set clearly improved the large error for the C−Cl distance (−0.0197 Å).

TABLE 6: Experimental Values[24] (Exp) and PCX Errors for a Selected Number of Bond Lengths (in Ångstrom) for the Four Polymorphs of NIC

	NIC−I		NIC−II		NIC−III		NIC−IV	
parameter	exp	PCX[a]	exp	PCX[a]	exp	PCX[a]	exp	PCX[a]
C_2–N_1	1.3522	−0.0273	1.3278	−0.0070	1.3439	−0.0252	1.3867	−0.0432
C_5–C_4	1.3745	0.0136	1.3731	0.0096	1.3833	−0.0002	1.3955	0.0244
C_6–N_1	1.3453	−0.0132	1.3308	−0.0071	1.3289	−0.0036	1.3259	0.0458
N_7–C_2	1.3541	0.0075	1.3669	−0.0002	1.3578	0.0102	1.3074	0.0251
C_8–N_7	1.4347	−0.0235	1.4022	−0.0049	1.4020	−0.0110	1.4013	0.0107
C_{10}–C_9	1.3943	−0.0028	1.3820	0.0030	1.3876	−0.0044	1.3626	0.0297
C_{11}–C_{10}	1.3585	0.0221	1.3834	0.0003	1.3920	−0.0065	1.3841	−0.0022
C_{12}–C_{11}	1.3625	0.0189	1.3761	0.0006	1.3668	0.0068	1.3930	−0.0158
C_{13}–C_8	1.3629	0.0263	1.3886	0.0018	1.3922	−0.0009	1.4081	−0.0224
C_{13}–C_{12}	1.3826	−0.0024	1.3852	−0.0046	1.3863	−0.0007	1.3263	0.0537
C_{14}–C_9	1.4888	0.0178	1.5038	0.0062	1.4987	0.0116	1.5189	−0.0094
O_{17}–C_{15}	1.2115	−0.0110	1.2326	−0.0205	1.2293	−0.0199	1.2326	0.0055
Cl_{18}–C_{10}	1.7261	0.0382	1.7453	0.0001	1.7450	0.0099	1.7256	0.0212

[a] PCX errors given as length_{PCX} minus length_{Exp}.

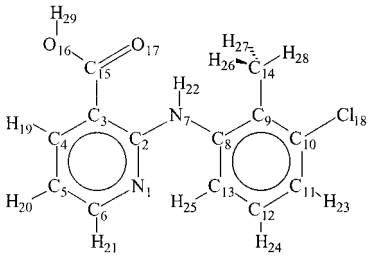

Figure 4. 2-(2-Methyl-3-chloroanilino) nicotinic acid (NIC−III).

Although the standard deviation for bond lengths did not change significantly, the angles did improve slightly over the PCX results.

The errors for the PCX model are comparable to those for the SM model. The SMX-15 results show only a marginal improvement over the SM results. The SMX-11 results show that the number of neighbors can be decreased successfully, the results being of the same quality as for the SMX-15 model.

III.2. Use of the PCX Model in a Study of the Geometry of 2-(2-Methyl-3-chloroanilino) Nicotinic Acid in its Four Polymorphic Forms. In the solid state, 2-(2-methyl-3-chloroanilino) nicotinic acid (NIC) exhibits conformational polymorphism. It can crystallize in four forms that will be numbered according to the Cambridge Structural Database (codes BIXGIY, BIXGIY02, BIXGIY03, and BIXGIY04): NIC−I through NIC−IV.

Space group properties and experimental lattice parameters[24] are summarized in Table 4. NIC-IV appears in the crystal state in a zwitterionic form, whereas the other polymorphs are nonionized. The four forms differ conformationally primarily in the relative arrangement of their two aromatic rings (Figure 4). The experimental values, for example, the C_9–C_8–N_7–C_2 torsion angles in NIC−I through NIC−IV are 71.27°, 160.24°, 178.81°, and −140.26°, respectively.

Franckaerts et al.[25] studied the four polymorphs of this molecule using the PC model. This model clearly showed its shortcomings, however. NIC−I and NIC−IV were not optimizable using this model. Furthermore, the PC model was not able to keep NIC−III in its planar crystal conformation and reverted to a nonplanar, gas-phase resembling conformation.

Using the PCX model, however, it was possible to optimize all four polymorphs. Moreover, the geometry optimization of NIC−III resulted in the planar structure in accordance with experimental results.

Results from the calculations on the yellow form of dimethyl 3,6-dichloro-2,5-dihydroxyterephthalate showed that the description of a chlorine atom needed a basis set with polarization functions. Therefore, the results presented in Tables 5−8 were obtained using the (6-)6-31G** basis set. The experimental values were also obtained from X-ray measurements at room temperature, so no structural parameters involving hydrogen atoms were included.

For NIC−I, NIC−II, and NIC−IV large errors arise for torsion angles, especially the torsion around the C_{15}–C_3 bond. This results in the COO(H) structures not being in the plane of the ring to which they are bonded.

Overall, the largest errors are found for NIC−IV. This might be because this structure is a zwitterion and diffuse functions should be included in the basis set describing these structures. Another reason might be the fact that the X-ray structure of this polymorph could not be determined as accurately as the other polymorphs because of the small size of the crystal used.[24]

All polymorphs have an intramolecular hydrogen bond between N_7–H_{22} and O_{17} constructing a six-membered ring. The distances between the donor and acceptor atoms for the experimental structures are 2.634, 2.702, 2.667, and 2.578 Å, respectively. The corresponding distances obtained with the PCX model are 2.697, 2.749, 2.676, and 2.562 Å. In NIC−I and NIC−II, the errors on the torsion angle around the C_{15}–C_3 bond cause a slight weakening of this hydrogen bond. The intramolecular donor−acceptor distances in hydrogen bonds in polymorphs NIC−III and NIC−IV are reproduced very well by the PCX model.

All polymorphs also have intermolecular hydrogen bonds. The experimental structure of NIC−I shows an intermolecular hydrogen bond between O_{16}–H_{29} and N_1, with a donor−acceptor distance of 2.710 Å. The PCX model shows a slightly weaker bond with a distance of 2.777 Å.

For NIC−II and NIC−III, two intermolecular hydrogen bonds have been found in the experimental structures. In these structures, the COOH groups point to each other, creating two O_{16}–H_{29}...O_{17} hydrogen bonds with donor−acceptor distances of 2.649 and 2.694 Å, respectively. For the PCX model, these distances are 2.670 and 2.656 Å. Again, for NIC−II the distances are a bit longer for the PCX model.

In NIC−IV, one intermolecular hydrogen bond is found. It is formed between N_1–H_{19} and O_{16} with a donor−acceptor distance of 2.753 and 2.733 Å for the experimental and PCX structure, respectively.

TABLE 7: Experimental Values[24] (Exp) and PCX Errors for a Selected Number of Valence Angles (in degrees) for the Four Polymorphs of NIC

	NIC−I		NIC−II		NIC−III		NIC−IV	
parameter	exp	PCX[a]	exp	PCX[a]	exp	PCX[a]	exp	PCX[a]
$C_3–C_2–N_1$	121.34	−0.14	122.04	−0.51	121.00	0.25	115.69	1.96
$C_6–N_1–C_2$	118.04	1.50	118.76	0.82	118.29	0.99	122.85	0.54
$C_6–C_5–C_4$	118.43	−1.19	118.47	−0.82	117.71	−0.58	117.99	−0.54
$C_5–C_6–N_1$	123.94	−0.17	123.36	0.28	124.96	−0.62	122.61	−1.77
$N_7–C_2–N_1$	118.04	0.51	117.42	1.21	119.43	0.10	122.30	0.24
$N_7–C_2–C_3$	120.62	−0.38	120.54	−0.72	119.57	−0.36	122.00	−2.19
$C_8–N_7–C_2$	125.22	1.33	132.27	−1.98	132.30	−0.25	131.95	−2.33
$C_9–C_8–N_7$	120.05	1.44	117.17	−0.81	115.34	0.48	118.01	1.38
$C_{10}–C_9–C_8$	116.39	−0.03	116.46	0.44	116.76	0.13	118.81	−3.08
$C_{11}–C_{10}–C_9$	122.29	1.25	123.57	−0.39	123.12	0.63	121.26	2.40
$C_{12}–C_{11}–C_{10}$	119.65	−1.11	118.06	0.57	118.44	−0.35	117.41	1.57
$C_{13}–C_8–N_7$	118.02	−0.36	121.42	1.75	124.08	0.18	121.09	−1.70
$C_{13}–C_8–C_9$	121.84	−1.13	121.35	−0.91	120.58	−0.68	120.83	0.27
$C_{13}–C_{12}–C_{11}$	120.25	−0.29	121.41	−0.87	121.28	−0.42	124.45	−4.93
$C_{12}–C_{13}–C_8$	119.50	1.22	119.09	1.22	119.79	0.71	117.16	3.75
$C_{14}–C_9–C_8$	122.04	−0.49	120.36	0.06	121.15	−1.30	121.10	1.90
$C_{14}–C_9–C_{10}$	121.57	0.51	123.15	−0.47	122.09	1.16	120.09	1.17
$O_{16}–C_{15}–C_3$	114.90	−1.47	114.54	−1.51	114.83	−1.01	113.93	1.67
$O_{17}–C_{15}–C_3$	123.02	0.99	123.57	1.63	123.35	0.80	116.14	0.16
$Cl_{18}–C_{10}–C_9$	119.63	0.10	119.84	0.54	120.18	0.34	122.03	−2.43
$Cl_{18}–C_{10}–C_{11}$	118.08	−1.36	116.57	−0.13	116.70	−0.97	116.67	0.07

[a] PCX errors given as angle_{PCX} minus angle_{Exp}.

TABLE 8: Experimental Values[24] (Exp) and PCX Errors for a Selected Number of Torsion Angles (in degrees) for the Four Polymorphs of NIC

	NIC−I		NIC−II		NIC−III		NIC−IV	
parameter	exp	PCX[a]	exp	PCX[a]	exp	PCX[a]	exp	PCX[a]
$C_4–C_3–C_2–N_7$	−179.30	−4.09	−179.68	−2.68	−179.04	−1.20	178.38	3.25
$C_{15}–C_3–C_2–N_1$	178.59	−4.64	−179.75	0.05	−176.48	−0.61	176.53	3.07
$C_{15}–C_3–C_2–N_7$	−0.46	−6.57	1.11	−2.51	3.42	−1.37	−2.65	1.42
$C_5–C_4–C_3–C_{15}$	−179.74	4.00	−179.43	−0.93	176.99	0.24	−177.55	−1.17
$N_1–C_6–C_5–C_4$	1.20	−2.76	2.45	−3.39	1.85	−1.17	−2.69	4.11
$C_8–N_7–C_2–N_1$	3.18	−8.23	−0.70	−5.89	1.14	−2.73	−0.89	−6.58
$C_8–N_7–C_2–C_3$	−177.74	−6.36	178.49	−3.44	−178.76	−1.99	178.23	−4.82
$C_9–C_8–N_7–C_2$	71.27	−1.69	160.24	1.10	178.81	1.90	−140.26	11.20
$C_{13}–C_8–N_7–C_2$	−111.94	−2.72	−22.23	1.76	−0.60	2.48	42.66	12.31
$Cl_{18}–C_{10}–C_9–C_{14}$	−3.51	−2.50	−2.50	3.05	−0.66	−2.28	0.86	−1.06
$O_{16}–C_{15}–C_3–C_2$	179.12	−4.36	−176.99	12.25	−177.50	−0.68	−178.76	−10.29
$O_{16}–C_{15}–C_3–C_4$	−2.06	−6.92	3.82	12.42	4.98	−0.83	0.22	−12.16
$O_{17}–C_{15}–C_3–C_2$	−1.02	−6.02	3.33	11.10	3.29	−0.87	0.40	−7.55
$O_{17}–C_{15}–C_3–C_4$	177.79	−8.56	−175.86	11.27	−174.23	−1.02	179.37	−9.41

[a] PCX errors given as angle_{PCX} minus angle_{Exp}.

IV. Conclusion

To study cases for which the PC model shows definite shortcomings and the SM model proved too expensive, the new PCX model was implemented. The SMX model was implemented because of possible improvements upon the SM model.

Both models were tested on formamide oxime, α-glycine, and the yellow form of dimethyl 3,6-dichloro-2,5-dihydroxyterephthalate. The PCX model was successfully applied to the geometry optimization of the four polymorphs of 2-(2-methyl-3-chloroanilino) nicotinic acid.

The PCX model, which is as fast as the PC model, proved to give results of SM quality. Using adequate force-field parameters, this model is a viable alternative for the SM model. Intra- and intermolecular hydrogen bonds are reproduced very well with the PCX model.

Further improvement in accuracy over the SM model can be achieved using the SMX model. Moreover, since the number of neighboring molecules included in the wave function can be reduced in the SMX model, computer times can be decreased without sacrificing accuracy.

Acknowledgment. B. S. and J. V. D. thank the Flemish governmental institution IWT for a predoctoral grant. This research was supported by the University of Antwerp under GOA-BOF-UA-23.

Supporting Information Available: Tables 1S−17S contain Cartesian coordinates for all optimized structures presented in this article. Tables 18S−21S contain all parameters used. This material is available free of charge via the Internet at http://pubs.acs.org.

References and Notes

(1) Peeters, A.; De Maeyer, E. A. P.; Van Alsenoy, C.; Verbeeck, R. M. H. *J. Phys. Chem. B* **1997**, *101*, 3995.

(2) Peeters, A.; Van Alsenoy, C.; March, N. H.; Klein, D. J.; Van Doren, V. E. *J. Phys. Chem. B* **2001**, *105*, 10546.

(3) Saebo, S.; Klewe, B.; Samdal, S. *Chem. Phys. Lett.* **1983**, *97*, 499.

(4) Angyan, J. G.; Silvi, B. *J. Chem. Phys.* **1987**, *86*, 6957.

(5) Bridet, J.; Fliszar, S.; Odiot, S.; Pick, R. *Int. J. Quantum Chem.* **1983**, *24*, 687.

(6) Mombourquette, M. J.; Weil, J. A.; Mezey, P. G. *Can. J. Phys.* **1984**, *62*, 21.

(7) Popelier, P.; Lenstra, A. T. H.; Van Alsenoy, C.; Geise, H. J. **1988**, *42*, 539.
(8) Peeters, A.; Van Alsenoy, C.; Lenstra, A. T. H.; Geise, H. J. *Int. J. Quantum Chem.* **1993**, *46*, 73.
(9) Warshel, A.; Levitt, M. *J. Mol. Biol.* **1976**, *103*, 227.
(10) Singh, U. C.; Kollman, P. A. *J. Comput. Chem.* **1986**, *7*, 718.
(11) Field, M. J.; Bash, P. A.; Karplus, M. *J. Comput. Chem.* **1990**, *11*, 700.
(12) Mulliken, R. S. *J. Chem. Phys.* **1955**, *23*, 2343.
(13) Hirshfeld, F. L. *Theor. Chim. Acta* **1977**, *44*, 129.
(14) Rousseau, B.; Peeters, A.; Van Alsenoy, C. *Chem. Phys. Lett.* **2000**, *324*, 189.
(15) Verwer, P.; Leusen, F. J. J. *Rev. Comput. Chem.* **1998**, *12*, 327.
(16) Gdanitz, R. J. *Curr. Opin. Solid State Mater. Sci.* **1998**, *3*, 414.
(17) van Eijck, B. P.; Mooij, W. T. M.; Kroon, J. *J. Comput. Chem.* **2001**, *22*, 805.
(18) Van Alsenoy, C.; Peeters, A. *THEOCHEM-J. Mol. Struct.* **1993**, *105*, 19.
(19) Brooks, B. R.; Bruccoleri, R. E.; Olafson, B. D.; States, D. J.; Swaminathan, S.; Karplus, M. *J. Comput. Chem.* **1983**, *4*, 187.
(20) Van Alsenoy, C. *J. Comput. Chem.* **1988**, *9*, 620.
(21) Peeters, A.; Van Alsenoy, C.; Lenstra, A. T. H.; Geise, H. J. *THEOCHEM-J. Mol. Struct.* **1994**, *110*, 101.
(22) Peeters, A.; Van Alsenoy, C.; Lenstra, A. T. H.; Geise, H. J. *J. Chem. Phys.* **1995**, *103*, 6608.
(23) Peeters, A.; Lenstra, A. T. H.; Van Doren, V. E.; Van Alsenoy, C. *THEOCHEM-J. Mol. Struct.* **2001**, *546*, 17.
(24) Takasuka, M.; Nakai, H.; Shiro, M. *J. Chem. Soc., Perkin Trans. 2* **1982**, 1061.
(25) Franckaerts, K.; Peeters, A.; Lenstra, A. T. H.; Van Alsenoy, C. *Electron. J. Theor. Chem.* **1997**, *2*, 168.
(26) Halgren, T. A. *J. Comput. Chem.* **1996**, *17*, 490.
(27) Francl, M. M.; Pietro, W. J.; Hehre, W. J.; Binkley, J. S.; Gordon, M. S.; Defrees, D. J.; Pople, J. A. *J. Chem. Phys.* **1982**, *77*, 3654.
(28) Gordon, M. S.; Binkley, J. S.; Pople, J. A.; Pietro, W. J.; Hehre, W. J. *J. Am. Chem. Soc.* **1982**, *104*, 2797.
(29) Pulay, P.; Fogarasi, G. *J. Chem. Phys.* **1992**, *96*, 2856.
(30) Fogarasi, G.; Zhou, X. F.; Taylor, P. W.; Pulay, P. *J. Am. Chem. Soc.* **1992**, *114*, 8191.
(31) Pulay, P.; Fogarasi, G.; Pang, F.; Boggs, J. E. *J. Am. Chem. Soc.* **1979**, *101*, 2550.
(32) Jeffrey, G. A.; Ruble, J. R.; McMullan, R. K.; Defrees, D. J.; Pople, J. A. *Acta Crystallogr., Sect. B* **1981**, *37*, 1381.
(33) Kvick, Å. *personal communication (neutron measurement at 15K).*
(34) Yang, Q. C.; Richardson, M. F.; Dunitz, J. D. *Acta Crystallogr., Sect. B* **1989**, *45*, 312.
(35) Richardson, M. F.; Yang, Q. C.; Novotnybregger, E.; Dunitz, J. D. *Acta Crystallogr., Sect. B* **1990**, *46*, 653.